

Simulating Damage due to a Lightning Strike Event: Effects of Temperature Dependent Properties on Interlaminar Damage

Paria Naghipour, Evan J. Pineda and Steven M. Arnold

NASA Glenn Research Center, 21000 Brookpark Rd., Cleveland, OH 44135

Abstract: *A multidirectional, carbon fiber/epoxy, composite panel is subjected to a simulated lightning strike, within a finite element method framework, and the effect of material properties on the failure (delamination) response is investigated through a detailed numerical study. The numerical model of the composite panel consists of individual homogenized plies with user-defined, cohesive interface elements between them. Lightning strikes are simulated as an assumed combination of excessive heat and high pressure loadings. It is observed that the initiation and propagation of lightning-induced delamination is a significant function of the temperature dependency of interfacial fracture toughness. This dependency must be defined properly in order to achieve reliable predictions of the present lightning-induced delamination in the composite panel.*

Keywords: *Composites, Delamination, Cohesive Zone Modeling, Lightning, Damage, Fracture, Heat Transfer, Crack Propagation.*

1. Introduction

Carbon fiber reinforced polymers (CFRPs) offer significant weight and performance advantages over metals, making them ideal for aerospace applications. However, CFRPs are dielectric (compared to highly conductive metals, such as aluminum); thus when subjected to an electrical impulse (such as a lightning strike) the electricity is not conducted through the CFRP structure. Consequently, the energy from the lightning strike is transformed to thermal energy through resistive super-heating of a highly localized region of the structure near the arc attachment point(s). The extreme surface temperatures induced by the lightning, along with an accompanying high-pressure shockwave (caused by rapid super-heating of the air surrounding the arc) yields extensive visible damage near the arc attachment point, as well as damage away from the arc attachment point that may not be detected through visual inspection. Thus, major damage in laminated composite aerospace structures is induced by direct effects of lightning during flight, affecting aircraft durability and long-term operation. In addition to direct effects associated with physical damages of lightning, indirect effects of lightning such as interferences with the electric system of the aircraft due to electromagnetic coupling are also hazardous (Chemartin, 2012). Therefore, airplanes should be protected against both direct and indirect effects of lightning. This paper focuses on the direct effects of lightning, which are of primary concern with the increased use of composites in aerospace industry.

The strike zone (red zone, Figure 1) is the major visible damage zone after a composite panel is hit by a lightning strike. Excessive surface temperatures cause major visible damage such as fiber sublimation and matrix pyrolysis (material recession) and delamination in this area. This strike zone and some area beneath this zone (the blue repair zone in Figure 1) are fully removed and replaced during regular inspection procedures.

However, a major area of concern is the residual zone (yellow zone, Figure 1), which is not repaired or replaced after inspection, but might contain highly-damaged areas due to lightning. As a result of a lightning strike, some regions in the residual zone are exposed to very high temperatures (much higher than matrix T_g), causing major degradation of matrix, fiber, and the interface. Furthermore, exposure of the matrix to such temperatures may increase the susceptibility of the composite to creep deformation during normal service hours.

Consequently, delaminations and inelastic matrix deformations are among the major damage mechanism occurring in this zone. However, these sub-critical damages are not easily detected during regular visual inspections, thus they may not be fully included in the repair zone. Accumulation of damage in overlapping residual zones, over multiple lightning strike events, might unexpectedly impact the structural performance of the composite panel significantly. Therefore, it is crucial to have an accurate estimate of the size of the actual damaged area, so that repairs can be completed properly, avoiding any unexpected catastrophic failure. Consequently, the repair zone (blue zone, Figure 1) might have to be redefined based on numerical predictions of the extent of the accumulated damage in the residual zone.

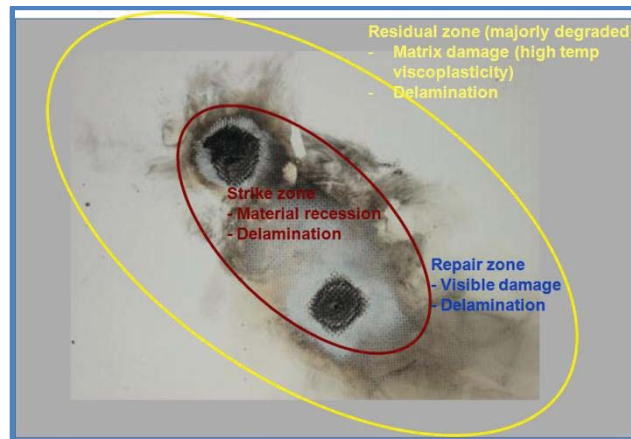


Figure 1. Damage resulting from simulated lightning strike experiment (courtesy of NASA Langley Research Center (LaRC)).

Although a predictive numerical tool can provide valuable information on the extent of the lightning-induced delamination damage in the residual zone, developing a competent numerical tool is a very challenging task. Available studies regarding simulated lightning strikes on composite panels are extremely limited (Feraboli, 2009; Featherston, 2010; Hirano, 2010;

Ogasawara, 2010; Kawakami, 2011; Chemartin, 2012), with almost no attempt to model the damage induced by lightning in CFRPs. Meanwhile, the variation of CFRP properties with high temperatures induced by lightning and the influence of these properties on lightning-induced damage remains largely unknown.

Starting with one of the most extensive available experimental studies, a series of simulated lightning strike experiments was conducted on un-notched and filled-hole carbon/epoxy laminates, and the damage area was evaluated via ultrasonic scanning, and advanced optical microscopy to gain further understanding of the morphology of damage (Feraboli, 2009). The authors were able to detect the damaged areas successfully for both types of specimens, with filled-holed specimens being extremely prone to delaminations. Later the effect of repair procedure on the structural performance of wire-mesh protected scarf-repaired carbon/epoxy specimens following a lightning strike was evaluated (Kawakami, 2011). According to the authors (Kawakami, 2011), a poor repair performs equally or worse, when subjected to a subsequent lightning strike, than a fully unprotected specimen, and therefore the damage margin (the region to be repaired) has to be defined precisely. Yet, another experimental study has addressed the evolution of damage in graphite/epoxy composite laminates due to lightning strikes with variations in lightning parameters and specimen size (Hirano, 2010). Ultrasonic testing, sectional observation and micro X-ray inspections were used to assess the damage, which was mainly categorized into fiber damage, resin deterioration, and internal delamination modes. The results showed that the lightning tests created large delaminations propagating in the shape of a pair of fans starting from the lightning attachment point in each interlayer. In addition to delamination, matrix cracks were also observed, however delamination was emphasized as the dominant failure mode among the others. The experiments also demonstrated that variation of specimen geometry has little effect on the lightning-induced damage response, while loading parameters such as peak lightning current or electric charge show distinct correlations with particular damage modes (Hirano, 2010). Later a finite element method (FEM) coupled thermal–electrical analysis of carbon fiber reinforced polymer composites (CFRP) exposed to simulated lightning current was carried out, in order to investigate the damage behavior caused by lightning strike (Ogasawara, 2010). In this study, the delamination area was estimated to be the same as matrix decomposition area (the areas where the temperature was $> 300\text{ }^{\circ}\text{C}$), as delamination was assumed to occur because of matrix decomposition accompanied by dielectric breakdown of pyrolysis gases. However, no actual progressive, continuum delamination modeling was accomplished within the FEM simulation (Ogasawara, 2010).

Based on the aforementioned literature (Feraboli, 2009; Featherston, 2010; Hirano, 2010; Ogasawara, 2010; Kawakami, 2011; Chemartin, 2012), delamination can be considered the most significant failure mode induced by a lightning strike, but it is difficult to detect through visual inspections. When inter-laminar damage (delamination) is the dominant failure mechanism, one recent appealing technique used in capturing delamination is the cohesive zone approach (Ortiz, 2009; Ladeveze, 2000; Alfano, 2001; Serebrinsky, 2005; Allix, 2006; Xie, 2006; Turon, 2007; Naghipour, 2011). The cohesive zone approach uses interface elements incorporating various traction-separation laws to capture crack initiation and propagation. Since the lightning phenomenon is assumed to be a combination of extreme temperatures and a pressure shockwave

leading to extensive inter-laminar damage, the cohesive laws should be reformulated to additionally account for thermal effects.

A comprehensive numerical model to predict the amount of lightning-induced delamination in the residual zone is currently not available in the mentioned literature. As the physical phenomenon behind a lightning strike is a very complicated one, a step-by-step methodology shall be followed to devise a general modeling tool for lightning-induced delamination prediction. The first step, which is the major focus of this work, is a systematic sensitivity study to present the effect of temperature-dependent parameters on the delamination progress, utilizing a temperature-dependent cohesive zone formulation.

Following this introduction, constitutive equations of the temperature-dependent cohesive user element are explained concisely. Construction of the numerical model, required input parameters, and various patterns of temperature dependency for these parameters are described in Section 3. Numerical simulations of the conducted lightning-induced delamination are presented in Section 4, and the obtained results are discussed. Finally, a brief summary and conclusion is presented in Section 5.

2. Cohesive Zone Model

The numerical FE model consists of individual elastic, transversely isotropic plies and interface elements between them as shown schematically in Figure 2. As in-ply damage is considered to be less significant based on available experimental evidence (Feraboli, 2009; Featherston, 2010; Hirano, 2010; Ogasawara, 2010; Kawakami, 2011; Chemartin, 2012), the only damageable portion is considered to be the interface. The mathematical damage model used for modeling interfacial damage in this work is implemented as a User Element in the FEM code Abaqus (Naghipour, 2011), and is described briefly in this section.

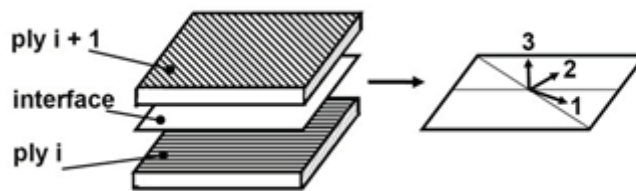


Figure 2. Schematic of lamina and interface elements in the FEM model.

The pursued mixed-mode cohesive element formulation is based on the constitutive models suggested in the literature (Ortiz, 1999; Turon, 2007) and is further modified to consider the temperature dependence of interfacial properties. Figure 3 shows the global and local geometries of the three-dimensional, 8-noded, zero-thickness interface element, which are related through the standard isoparametric mapping. Nodes 1-4 represent lower face of the interface and nodes 5-8, which coincide geometrically with nodes 1-4, represent the upper surface. (The zero thickness has been offset for better visualization).

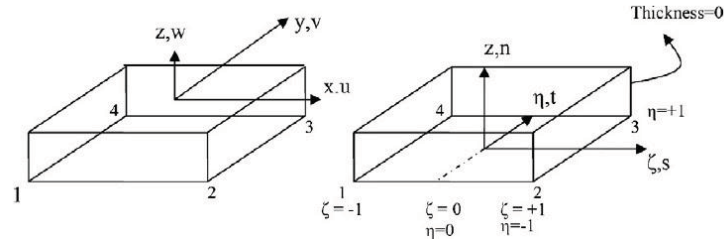


Figure 3. Interface element with global and local coordinate systems.

With respect to the three-dimensional global coordinate system, x, y, z , each node has three degrees of freedom, u, v and w respectively. Meanwhile, in the local coordinate system the vector of relative displacements between each pair of the corresponding upper and lower nodes of the element is defined as:

$$\begin{bmatrix} \delta_n \\ \delta_s \\ \delta_t \end{bmatrix} = \begin{bmatrix} u_n \\ u_s \\ u_t \end{bmatrix}_{TOP} - \begin{bmatrix} u_n \\ u_s \\ u_t \end{bmatrix}_{BOTTOM} \quad (1)$$

n indicates the opening or normal component and s and t indicate the two shear components, respectively, as shown in Figure 3. The mixed-mode damage formulation is based on constitutive interface tractions (τ_n, τ_s, τ_t) and relative displacements ($\delta_n, \delta_s, \delta_t$) (Figure 4).

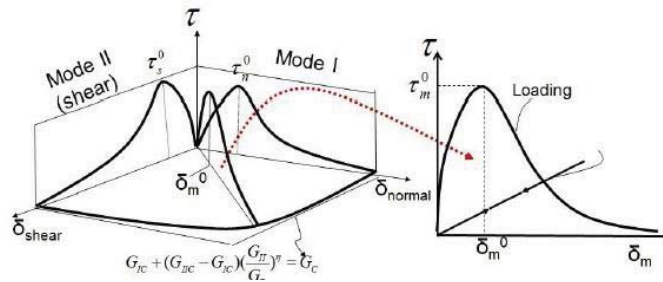


Figure 4. Mixed-mode traction separation law for the cohesive element.

Interfacial damage initiates upon satisfaction of the quadratic interfacial traction interaction criterion as shown in Equation (2). The relative displacement corresponding to damage initiation

in the mixed-mode plane, δ_m^0 (Figure 4), is called the mixed mode opening displacement of the fictitious crack tip.

$$\left(\frac{\tau_n}{\tau_n^0(\theta)}\right)^2 + \left(\frac{\tau_s}{\tau_s^0(\theta)}\right)^2 + \left(\frac{\tau_t}{\tau_t^0(\theta)}\right)^2 = 1 \quad (2)$$

τ_n^0 , τ_s^0 , τ_t^0 are the normal and shear elastic limits of the interface, which are assumed to vary linearly with temperature (Θ). Once the damage is initiated, it starts evolving based on an energy based propagation criterion given by Benzeggagh and Kenane (B-K) (Benzeggagh, 1996):

$$G_{IC}(\theta) + (G_{IIC}(\theta) - G_{IC}(\theta)) \left(\frac{G_{shear}(\theta)}{G_T(\theta)} \right)^\eta = G_C(\theta) \quad (3)$$

$$G_T(\theta) = G_I(\theta) + G_{shear}(\theta)$$

Note, that the form of both the initiation criterion (Equation (2)) and the mixed-mode propagation criterion (Equation (3)) are based upon empirical observations. It is assumed that these forms are adequate for this material system, and testing this hypothesis is beyond the scope of this work. Future experimental studies will be conducted to determine if Equations (2) and (3) can sufficiently fit experimental data under a variety of temperatures and mixed-mode conditions.

$G_{IC}(\Theta)$ and $G_{IIC}(\Theta)$ are temperature-dependent fracture toughness values for mode I and mode II that must be determined from fracture experiments conducted at various temperatures. The mixed-mode failure response of the material is described by plotting the total critical fracture toughness G_c vs. different mode mixities (G_{shear}/G_T). Parameter η in Equation (3) maintains the shape of the failure locus in the mixed-mode plane, and the most accurate failure criterion is the one matching the material response when plotted in this mixed mode diagram. As the damage evolves based on the mentioned energy-based criterion, an isotropic damage variable, d , (Equation 4) degrades the interfacial tractions, until the final separation point (δ_m^f in Figure 4) is reached. The damage variable (d) degrading the interfacial tractions is calculated at the end of each increment and is recorded to indicate the initialization and the extent of propagated damage in interface elements.

$$d = \frac{e \tau_m^0 \delta_m^0 \left[1 - \left(1 + \frac{\delta_m^{\max}}{\delta_m^0} \right) e^{-\delta_m^{\max} / \delta_m^0} \right]}{G_C} \quad (4)$$

3. FE Model Description and Input Material Properties

The numerical model was created using the object oriented Abaqus scripting interface for further optimization and parametric studies. The laminate is a 500 mm x 500 mm square composite panel, made of 10 AS4/PEEK plies (1.4 mm thickness) with a quasi-isotropic stacking sequence and interface elements placed in between laminae. Each lamina is defined using elastic, transversely-isotropic, 8 node, reduced integration, continuum shell elements. The interface elements, implemented as user-defined elements (UEL) in Abaqus, are placed between the plies to capture the delamination behavior. When the panel is subjected to a lightning strike, the front surface temperature is estimated to be about 3900–4200 °C (Hirano, 2010; Ogasawara, 2010). However, the numerical simulations presented in Ogasawara (2010) contained a maximum applied temperature of 3000 °C, which is the fiber sublimation temperature. Above these temperature the composite material has completely ablated, and cannot transfer any heat; therefore, a maximum applied temperature of 3000 °C was also used in the simulations presented in this work (see Figure 5). Meanwhile a 50 kA strike is reported to create a shockwave with an approximate 20–30 MPa pressure in the vicinity of the attachment point (Hill, 1971; Featherston, 2010). Accordingly, loading boundary conditions (excessive surface temperatures and a pressure), are applied to the panel in a circular area (radius=10 mm depth= 0.4 mm) in the middle of the panel (Figure 5), and the edges are clamped. The area for application of the loads is determined based on experimental observations available in literature (Feraboli, 2009; Featherston, 2010; Hirano, 2010; Ogasawara, 2010; Kawakami, 2011; Chemartin, 2012) and the simulated lightning tests conducted at Lightning Technologies, Inc. (LTI) (Figure 1). The load is applied in a quasi-static manner in order to reduce further complexities caused by dynamic effects and only to focus on the influence of temperature variations on the delamination progress. However, dynamic effects are planned to be included in future studies. Note that the results of this study might also be reproduced using built-in Abaqus cohesive elements to be compared with the current results. However, because of the convenience of the UEL for further additions of pressure and subcritical delamination effects, and due to the long run times of the analysis this comparison is not addressed in this work.

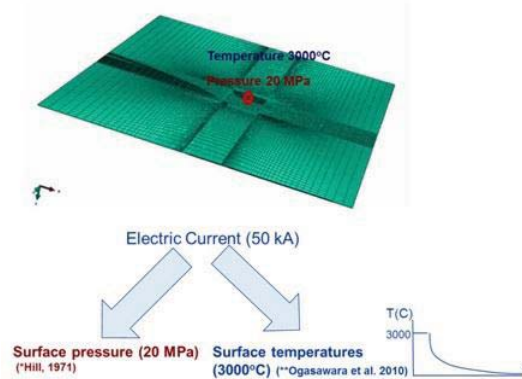


Figure 5. FE mesh of the composite plate and applied boundary condition

The material properties of the ply and interface (for room temperature) are listed in Table 1. Lamina properties, longitudinal and transverse ply stiffness (E_{11} , E_{22}), Poisson's ratio (ν_{12}), longitudinal and transverse shear modulus (G_{12} , G_{23}) and their variation with temperature are partially reported in literature (Kohlgruber, 1997). These ply properties are known to have very small temperature dependencies. In order to have a precise numerical model, directional thermal-conductivity data (K_{11} , K_{22} , K_{33}) should also be determined as a function of temperature through standardized conductivity experiments. Nevertheless, in order to purely focus on the influence of temperature-dependent *interfacial* properties on the lightning-induced damage response, these ply-specific properties have been assumed to remain constant in this study. In contrast to ply properties, very little, and moreover conflicting, data is available on variation of interfacial properties with temperature in the reported literature (Johnson, 1985; Reeder, 2002). Typical interface properties, which presumably vary with temperature, are normal and shear fracture toughness (G_{Ic} , G_{IIc}) and corresponding strength values (τ_n^0 , τ_s^0). The fracture toughness values at room temperature (listed in Table 1) are measured through available fracture experiments (Naghypour, 2011).

Table 1. Lamina/interface parameters at room temperature.

Mechanical Ply Properties						
E_{11} (MPa)	E_{22} (MPa)	ν_{12}	G_{12} (MPa)	G_{23} (MPa)	K_{11} (W/m/K)	$K_{22} = K_{33}$ (W/m/K)
138,000	10,500	0.3	6,300	3,500	11.8	0.609
Mechanical properties of interface at room temperature						
τ_n^0 (MPa)	$\tau_s^0 = \tau_t^0$ (MPa)	G_{Ic} (mJ/mm²)		G_{IIc} (mJ/mm²)		η
75	80	0.97		1.72		2.3

In order to thoroughly investigate the effect of temperature dependence of the delamination process, the modeling study has been divided into two categories. In the first category, three different temperature dependent profiles for interfacial fracture/ strength values have been assumed. Single mode and mixed mode fracture toughness and strength values (G and τ) experience a linear reduction to 80%, 40% and 20% of their room temperature values, as the temperature rises from room temperature to 4000 °C (See Figure 6a). In the second category, mixed mode fracture toughness and strength values experience a linear reduction to 80%, 40% and 20% of their room temperature values, when the temperature rises from room temperature to the glass transition temperature ($T_g \sim 190$ °C) (see Figure 6b). For temperatures higher than T_g , the corresponding toughness and strength values are assumed to be close to zero.

Note that, assuming different temperature dependent profiles with higher/lower rates of reduction will undoubtedly yield different delamination responses. The profiles here are just initial assumptions, and are not representative of any experimental data. The main focus is to emphasize the significance of temperature-dependent interfacial properties on lightning-induced delamination response via employing a generic temperature dependence profile. In order to determine precisely the temperature-dependent fracture toughness values, fracture experiments must be conducted under various temperatures, and corresponding fracture loads and crack propagation data must be recorded. However, obtaining fracture data in elevated temperature ranges is a challenging task. Currently, no experimental standards exist for this, and no comprehensive experimental studies

have been conducted with definitive success. The results reported in a few studies addressing high temperature fracture testing (Johnson, 1985; Reeder, 2002) seem to be inconsistent and need further investigation. Hence, the results of this numerical study can avail as a firm incentive for further research planning on temperature-dependent fracture experiments.



Figure 6. Three assumed temperature dependent profiles for interfacial fracture/ strength values a) Temperature range from baseline to 4000C, b) Temperature range from baseline to T_g

4. Results and Discussion

A thorough parametric study has been conducted to understand the influence of various interfacial material parameters on the extent of damage induced by a lightning strike on an unprotected CFRP panel. The composite panel is subjected to assumed, lightning-induced, loading conditions as described in Section 3, and the delamination evolution is studied under the specified conditions.

4.1 Lightning-induced delamination; Three temperature dependent profiles (20%, 60% and 80% reduction in interfacial fracture/ strength values with a temperature change from baseline to 4000C)

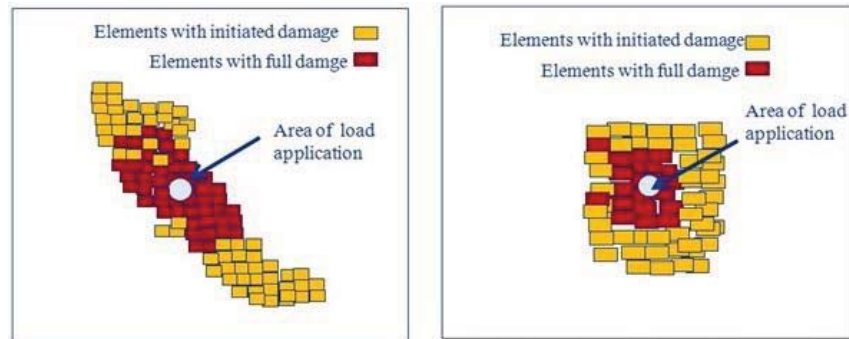
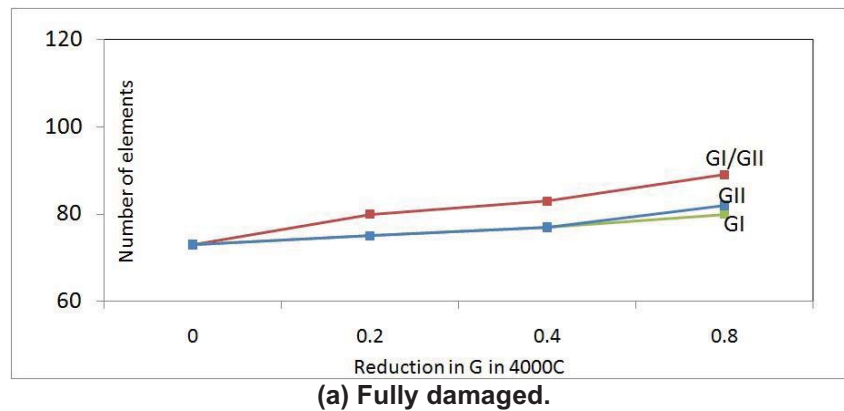


Figure 7. Delamination profiles: 80% linear descent in interfacial properties (strength and toughness) is assumed (left), no temperature dependency is assumed (right).

The importance of using accurate temperature-dependent interface properties to predict the lightning induced delaminations is demonstrated in Figure 7. Two various delamination profiles are compared with each other; one with no temperature dependency (right), and the other one with an 80% temperature-dependent linear descent in interface strength and toughness (left), when the temperature rises to 4000C. Semi fan-shaped delamination propagation is observed for the former, while we notice a homogenous propagation scheme in the latter case. Although the number of damaged elements in the delamination area might not exhibit a significant rise, the delamination profiles are completely different from each other. Based on observed delamination schemes, the mentioned repair zone (blue zone, Figure 1) might have to be redefined to avoid any structural failures.

As summarized in Figure 8, variation of mode I and mode II fracture toughness with temperature ($G_I(\theta)$ and $G_{II}(\theta)$) results in approximately the same change in the lightning-induced delamination. For example, with temperature-dependent fracture toughness (i.e., with the G_I value undergoing a 80%, 40% and 20% linear descent with temperature) the number of failed interface elements exhibit 10.9%, 4.1%, and 2.7% increase respectively, compared to the fixed G_I (see Figure 8a). Likewise, the same temperature-dependence definition in mode II or combined mode I/mode II fracture toughness produces similar results in the number of failed elements with a moderate difference of about 5% compared to G_I . The slow rate of descent in G (as a function of temperature) is assumed to be the cause of the apparent insensitivity of the resulting damage on the functional form of G . Assuming a faster descent rate would definitely result in a larger difference between the damaged elements obtained using the various temperature dependent fracture toughness profiles (as will be shown in Section 4.2).

A similar sensitivity of the number elements with initiated interfacial damage on the temperature dependent properties is observed (see Figure 8b). Elements with initiated damage are defined as those with a damage variable exceeding 0.5. It is clearly observed that the number of damage initiated elements exhibits a consistent, but not necessarily linear change with the variations in fracture toughness values. Hence, temperature-dependent fracture experiments should be performed to have a better understanding of the temperature-dependence of fracture toughness, and therefore have a better estimation of the extent of delamination induced by lightning.



Next, the influence of temperature-dependent interfacial strengths (τ_n^0 , τ_s^0) on the delamination zone induced by lightning has been studied. By applying an 80% linear descent (from room temperature to 4000 °C) in interfacial strength values with increasing temperature (assuming fixed and fracture toughness), the difference in the delamination zone size has been investigated. It is observed that, when keeping the fracture toughness fixed, changing the interfacial strength values with temperature has a small effect on the delamination area (Figure 9). Nevertheless, the number of elements with initiated damage is slightly higher, due to faster initiation of damage based on decreased interfacial strength values. The damage initiates but does not propagate thoroughly, as propagation is majorly driven by fracture toughness values. Thus, for the assumed strength degradation profiles, interfacial strengths do not play an important role on the size of the propagating delamination in absence of temperature-dependent fracture toughness variation.

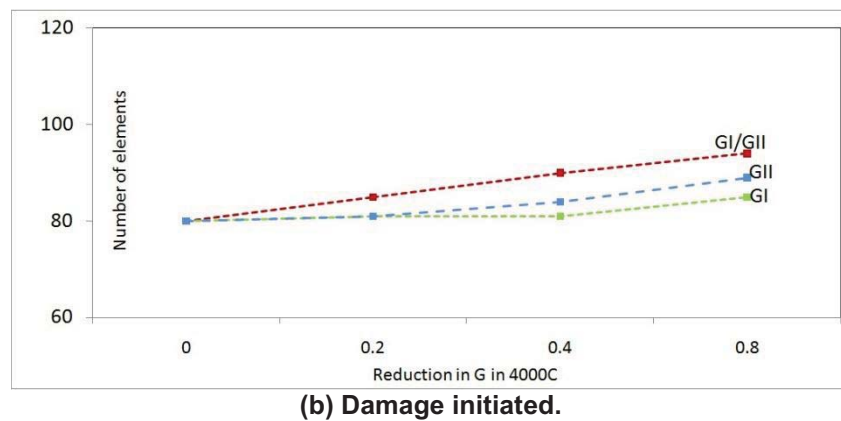


Figure 8. Number of damaged elements for variations in temperature-dependent fracture toughness

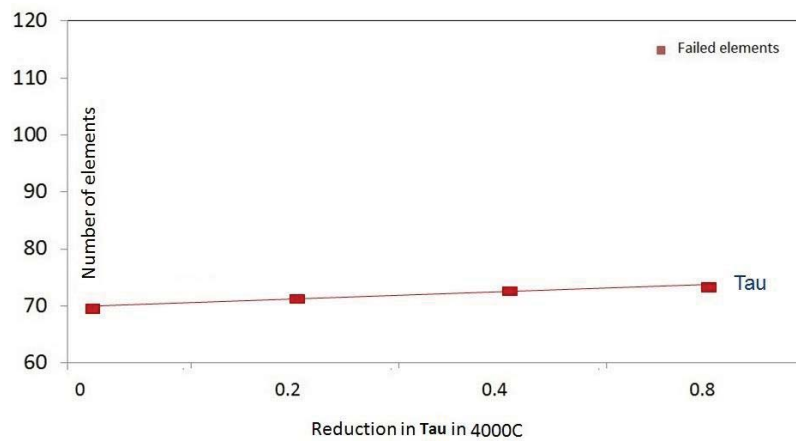
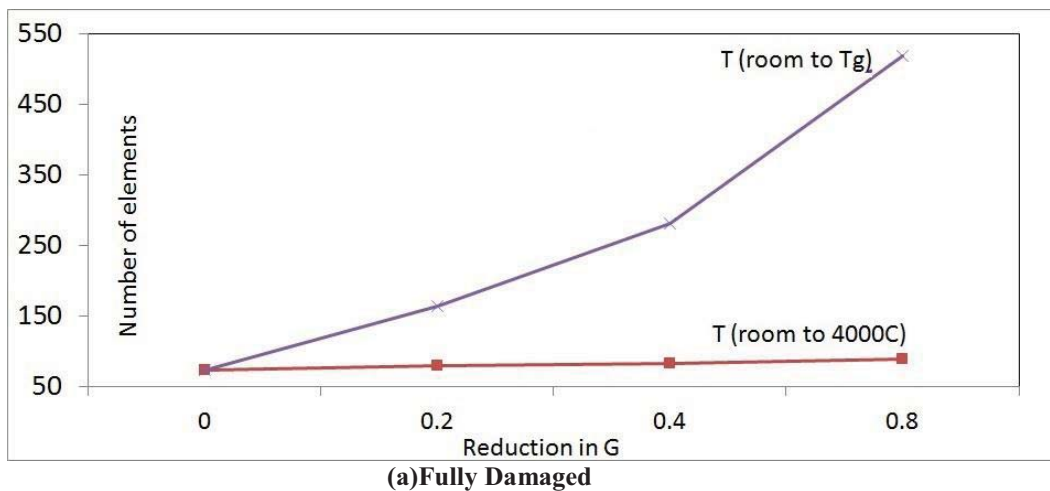


Figure 9. Number of failed elements for variations in temperature-dependent interfacial strength.

4.2 Lightning-induced; Three temperature dependent profiles (20%, 60% and 80% reduction in interfacial fracture/ strength values with a temperature change from baseline to Tg)



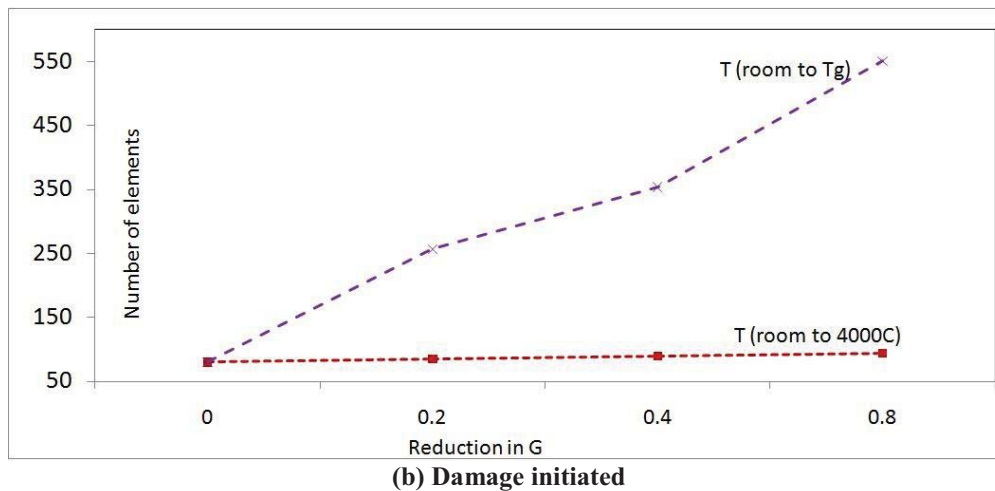


Figure 9. Comparison of number of damaged elements for various reduction rates of fracture toughness in interface elements

Figures 9a and 9b show that, the relative number of failed elements (Figure 9a), and damage initiated elements (Figure 9b) is significantly different, when the corresponding fracture toughness values are reduced by 20%, 40% and 80% as the temperature increases from room temperature to T_g . It is apparent that the number of failed elements, or elements with initiated damage, is significantly more sensitive to the temperature dependency of G when the reductions in mixed mode fracture toughness values are assumed to occur over temperatures ranging from room temperature to T_g (instead of room temperature to 4000C). For instance, the number of failed elements has been almost doubled, when a 80% reduction in G is assumed instead of a 20% reduction over the mentioned temperature range (room to T_g). In the former case (Figs 7a and 7b) this increase in the number of failed elements was only about 7%. Thus, it is further emphasized here that the correct definitions for the temperature dependent, interfacial parameter, degradation profiles are critical.

5. Conclusion

A numerical model, consisting of multidirectional plies with temperature-dependent cohesive interface elements in between, was subjected to lightning simulated as a combination of a mechanically applied pressure together with very high thermal gradients. A parametric study was carried out, i.e., corresponding interfacial parameters were varied over a definite temperature range, in order to understand their influence on the predicted lightning damage response. As a basis for comparison, the delamination (number of damaged interfacial elements) was recorded under the specified conditions. It is concluded that, interfacial fracture toughness is the primary parameter controlling lightning-induced delamination propagation, while varying interfacial strengths only changes the initiation of damage and does not influence the size of the propagating delamination. The size of the delamination is strongly dependent on the reduction rate of fracture

toughness values with temperature, as higher reduction rates produce a significantly greater number of failed interface elements. It is also observed that the shape of the delamination zone is a significant function of temperature-dependent fracture properties. Based on the shape of the delamination zone, regular repairs might have to be reconsidered to avoid sub-critical failures. Therefore, it can be concluded that measuring the temperature dependence of the fracture toughness is critical in order to predict the delaminated area resulting from a lightning strike. It is worth mentioning that this study is a preliminary study, and further complexities will be built up systematically to capture all the necessary physics and devise a robust lightning-induced damage prediction model.

6. References

1. Alfano, G., and M. A. Crisfield, "Finite Element Interface Models for Delamination Analysis of Laminated Composites," *International Journal for Numerical Methods in Engineering*, vol. 50, 1701-1736, 2001.
2. Allix, O., and L. Blanchard, "Mesomodeling of Delamination: Towards Industrial Applications," *Composites Science and Technology*, vol. 66, 731-744, 2006.
3. Benzeggagh M.L., and M. Kenane, "Measurement of Mixed-Mode Delamination Fracture Toughness of Unidirectional Glass/Epoxy Composites With Mixed Mode Bending Apparatus," *Composites Science and Technology*, vol. 56, 439-449, 1996.
4. Chemartin, L., P. Lalande, B. Peyrou, A. Chazottes, P. Q. Elias, C. Delalondre, B. G. Cheron, and F. Lago, "Direct Effects of Lightning on Aircraft Structure: Analysis of Thermal, Electric and Mechanical Constraints," *Lightning Hazards to Aircraft and Launchers*, *Journal Aerospace Lab*, issue 5, 78-91, 2012.
5. Featherston, C. A., M. Eaton, S. L. Evans, K. M. Holford, R. Pullin, and M. Cole, "Development of a Methodology to Assess Mechanical Impulse Effects Resulting from Lightning Attachment to Lightweight Aircraft Structures," *Applied Mechanics and Materials*, vol. 24-25, 129-134, 2010.
6. Feraboli, P., and M. Miller, "Damage Resistance and Tolerance of Carbon/Epoxy Composite Coupons Subjected to Simulated Lightning Strike," *Composites: Part A*, vol. 40, 954-967, 2009.
7. Hill, R. D., "Channel Heating in Return Strike Lightning," *Journal of Geophysical Research*, vol. 76, no. 3, 1971.
8. Hirano, Y., S. Katsumata, Y. Iwahori, and A. Todoroki, "Artificial Lightning Testing of Graphite/Epoxy Composite Laminate," *Composites: Part A*, vol. 41, 1461-1470, 2010.
9. Johnson, W. S., and P. D. Mangalgiri, "Influence of the Resin on Interlaminar Mixed-Mode Fracture," *NASA/TM-87571*, 1985.
10. Kawakami, H., and P. Feraboli, "Lightning Strike Damage Resistance and Tolerance of Scarf-Repaired Mesh-Protected Carbon Fiber Composites," *Composites: Part A*, vol. 42, 1247-1262, 2011.

11. Kohlgruber, D., "Mechanical In-Plane Failure Properties of PEEK/AS4," Internal Report, CYTEC/DLR Institute of Structures and Desing, German Aerospace Center-DLR, Stuttgart, 1997.
12. Ladaveze, P. L., L. Guitard, L. Champaney, and X. Aubard, "Debond Modeling for Multidirectional Composites," *Computation Methods in Applied Mechanics and Engineering*, vol. 183, no. 1-2, 109-122, 2000.
13. Naghipour, P., M. Bartsch, and H. Voggenreiter, "Simulation and Experimental Validation of Mixed Mode Delamination in Multidirectional CF/PEEK Laminates Under Fatigue Loading," *International Journal of Solids and Structures*, vol. 48, 1070-1081, 2011.
14. Ogasawara, T., Y. Hirano, and A. Yoshimurai, "Coupled Thermal-Electrical Analysis for Carbon Fiber/Epoxy Composites Exposed to Simulated Lightning Current," *Composite: Part A*, vol. 41, 973-981, 2010.
15. Ortiz, M. and A. Pandolfi, "Finite-Deformation Irreversible Cohesive Elements for Three-Dimensional Crack-Propagation Analysis," *International Journal of Numerical Methods in Engineering*, vol. 44, 1267-1282, 1999.
16. Reeder, J. R., "Prediction of Long-Term Strength of Thermoplastic Composites Using Time-Temperature Superposition," NASA/TM-2002-211781, 2002.
17. Serebrinsky, S., and M. Ortiz, "A Hysteretic Cohesive-Law Model of Fatigue-Crack Nucleation," *Scri Mater*, vol. 53, 1193-1196, 2005.
18. Turon, A., C.G. Davila, P. P. Camanho, and J. Costa, "An Engineering Solution for Mesh Size Effects in the Simulation of Delamination using Cohesive Zone Models," *Engineering Fracture Mechanics*, vol 74, 1665-1685, 2007.
19. Xie, D., and A. M. Waas, "Discrete Cohesive Zone Model for Mixed-Mode Fracture using Finite Element Analysis," *Engineering Fracture Mechanics*, vol. 73, 1783-1796, 2006.